

Use of electrolyte cathode glow discharge (ELCAD) for the analysis of complex mixtures†

Michael R. Webb, Francisco J. Andrade and Gary M. Hieftje*

Received 21st November 2006, Accepted 19th March 2007

First published as an Advance Article on the web 8th May 2007

DOI: 10.1039/b616989a

Use of an electrolyte-cathode glow discharge (ELCAD) with complex samples is explored. The present state of knowledge in this regard is briefly reviewed and several previously undocumented effects are examined. Remedies to various interferences are proposed and evaluated. The implications of the results to the mechanistic understanding of ELCAD are discussed.

1 Introduction

Inductively coupled plasma (ICP), particularly when coupled with mass spectrometric (MS) detection, is rightly recognized as a powerful tool for elemental analysis, but this power comes with significant costs. Both gas ($> 15 \text{ L min}^{-1}$ Ar) and power ($> 1 \text{ kW}$) consumption are high and, along with the need for vacuum equipment, effectively tie an ICP-MS to the laboratory. With these considerations in mind, it is easy to appreciate the continued use of other techniques (*e.g.* electrothermal vaporization atomic absorption and flame atomic absorption and emission) and the interest in development of new sources, particularly miniaturized ones.

Electrolyte-cathode discharge (ELCAD) is an alternative source for elemental analysis of liquid solutions first introduced by Cserfalvi *et al.* in 1993.¹ It has a small footprint, low power consumption ($< 75 \text{ W}$), and operates in atmospheric-pressure air. In essence, it is a glow discharge using an electrolytic solution as the cathode and a metal rod as the anode. The electrolytic solution serves as the sample in the ELCAD, just as the solid cathode often does in a conventional low-pressure glow discharge.

Despite its simplicity, the ELCAD performs quite well. Detection limits for a range of metals are generally in the 10s of ppb^{2,3} and short-term precision is typically around 1% for ppm concentrations (this work). One aspect that is in need of further study is how well complex solutions can be analyzed. For our purposes, complex solutions are samples that differ from standards in more ways than the concentration of the analyte being determined. Acidified tap water (often with additional metals added) has been used as the sample solution several times,^{1,3-9} but the concentrations measured by ELCAD have not been compared to those measured by other techniques. Similarly, acidified diluted milk (3 mL in 1 L) has been analyzed using ELCAD,⁷ but without comparison to known values.

Experience with flames and other plasmas suggests we should expect interferences of some sort. Such interferences should be studied to establish both the limitations of the

technique and ways to overcome those limitations when possible. Further, effects of concomitant species have sometimes provided insight into operational mechanisms of other techniques.^{10,11}

Before reporting the results of this study, it is worthwhile to review what is already known about analyzing complex samples with ELCAD.

1.1 Spectral interferences

Spectral interferences can be placed broadly into two categories: background emission and concomitant species emission. The former can impair performance, especially by constraining detection limits, but is not particular to complex samples. Rather, it is the latter that is relevant in the present context. Some sources, such as the ICP and the low-pressure glow discharge, are linerich, which increases the potential for spectral overlap. In the ELCAD, very little ionic emission is observed.^{12,13} The electron number density ($8.5 \times 10^{14} \text{ cm}^{-3}$) and the ionization temperature (5000 K) have been used to predict the degree of ionization for various elements in the plasma and found to be quite low for most elements (less than 10% for the majority of the 88 elements considered).¹² Low ionic emission is expected to make spectral overlap somewhat less common.

Recently, two studies^{2,8} have shown that the spatial distribution of analyte emission varies by element. It is possible that this feature could be exploited to reduce spectral interference, although the gains are unlikely to be worth the additional complexity.

1.2 Ionization interference

Ideally, the ratio of atoms to ions of an analyte should be unaffected by either the concentration of the analyte or the concentrations of other sample concomitants. If this is true, a calibration plot based on either the atom concentration or the ion population in the source (for example, on measuring atomic or ionic emission) will be useful for calculating concentrations of the element in the solution. In reality, this ratio is proportional to the electron number density (assuming that other plasma characteristics are unchanged).¹⁴ In a flame, the electron number density is affected significantly by electrons produced by the ionization of even low concentrations of metals because the background electron number density is comparatively low. This results in gas-phase atom and ion

Department of Chemistry, Indiana University, Bloomington, Indiana 47405-4001, USA

† The HTML version of this article has been enhanced with colour images.

populations (and therefore atom and ion emission and absorption) that are nonlinear with solution concentrations and are altered by the presence of other elements. In an ICP, the background electron number density is high enough (typically measured as around 10^{15} cm^{-3})¹⁴ that changes caused by elements in the sample solution are insignificant. As was previously mentioned, the electron number density in the ELCAD has been measured to be $8.5 \times 10^{14} \text{ cm}^{-3}$, nearly as high as the ICP. Given that, ionization interference would not be expected in an ELCAD. Supporting this, the same paper showed no evidence of this interference in an ELCAD under conditions where it would have been pronounced in a flame.¹²

1.3 Electrolyte effects

Early ELCAD experiments showed that pH has a strong effect on analyte emission.¹ To produce analyte emission from the ELCAD, a pH below about 2.5 is required, with a more acidic pH producing stronger emission. Over a pH range of 0.8 to 1.9, which roughly covers the practical range of the technique, emission decreases linearly five- to eight-fold for the elements studied in a recent paper.² Given that pH is a logarithmic scale, this translates to changes in acid concentration having relatively smaller effects on emission when the starting concentration is high than when it is low. For example, a 2 mM acid addition to a solution originally having a pH of 2 would shift the pH by 4%, but the same amount of acid added to a solution originally having a pH of 1 would only shift the pH by 0.9%. Since emission is linearly related to pH, the relative change in emission will be less for the pH 1 solution than the pH 2 solution. For this reason, and because of the increased emission, we recommend using a relatively low pH and typically use a pH of 1.

It has been shown that the supporting electrolyte identity has a significant effect on emission as well, and that electrolytes other than acids can be used. Mezei *et al.*¹⁵ found that using acids as the supporting electrolyte results in greater emission than using salts and that there is variation according to the acid anion. Specifically, they determined the sequence of analyte emission to be $\text{H}_2\text{SO}_4 < \text{HNO}_3 < \text{HCl}$ and suggested use of HCl. We suggest HNO_3 instead for reasons of chemical compatibility. Yagov and Gentsina¹⁶ had similar results for a source akin to the ELCAD, the drop-spark discharge (DSD). A DSD differs from an ELCAD in that the anode is also an electrolytic solution rather than a solid metal.

2 Experimental

The equipment used in this study has been diagrammed and described in detail previously,^{2,12} so only a brief description will be given here. The sample solution enters the cell through a portion of a 1-mL serological pipette that has been bent so the tip points upwards a few millimeters below a 1.6 mm diameter Ti anode. Except where noted, the gap was 3 mm. A Kepco (Flushing, NY) BHK 2000–0.1 MG or BHK 1000–0.2 MG high-voltage power supply operated in constant-current mode is connected to this anode through a 400 Ω ballast resistor. Unless otherwise noted, an 80 mA current was used. The sample solution overflows from the tip into an approximately 35 mL reservoir containing a grounded gra-

phite electrode. This overflow creates an electrical connection between the solution at the pipette's tip and the graphite electrode. Unless otherwise noted, the solution was acidified with nitric acid to pH 1. The discharge is initiated by bringing the anode close to the solution.

A black rectangular polyethylene divider supported by the pipette reduces the amount of hydrogen (produced at the graphite cathode) that reaches the discharge, blocks some light from sources external to the discharge, and wicks moisture over the sides of the reservoir so a constant solution level is maintained within the reservoir. The hydrogen is blocked because its presence is known to affect emission in other glow discharges;¹¹ the light is obstructed to reduce background noise; and the reservoir level is held constant to prevent fluctuations in the ohmic drop across the solution between the pipette tip and the graphite cathode.

The solution is supplied using a Global FIA MilliGAT (Fox Island, WA) flow-injection system. A six-port two-way switch allows the sample to be changed without interrupting the solution flow. The discharge is imaged at a magnification of 2.3 : 1 with a quartz lens onto the entrance slit of a Chromex (Albuquerque, NM) 500IS/SM 0.5 m Czerny–Turner spectrometer. Observation is limited to approximately the bottom two thirds of the discharge by using electrical tape affixed to the monochromator entrance slit. Detection is accomplished with a Hamamatsu (Hamamatsu, Japan) R928 PMT biased at –850 V, which feeds a Keithley (Cleveland, OH) 427 current amplifier. The output of this amplifier is recorded with a custom LabVIEW (National Instruments Corporation, Austin, Texas) program. Except where otherwise noted, emission intensities and standard deviations are based on ten consecutive measurements of the same sample, where each measurement is the averaged intensity from a 10-s period acquired at 1 kHz.

3 Results and discussion

3.1 Dynamic range

To minimize sample handling and thereby reduce the likelihood of contamination and the time needed to analyze a sample, it is preferable not to dilute the solution. A broad dynamic range makes dilution less likely to be necessary. The benefits of a large dynamic range are even greater for complex samples, as elements may be present at widely disparate concentrations and samples made through different degrees of dilution might otherwise be necessary. This is a particular problem in flame AAS, which typically has a linear range of only about two orders of magnitude.^{17–19}

To evaluate the dynamic range of ELCAD, calibration curves (shown as log–log plots in Fig. 1) were constructed for five elements (Ca, Cd, Cu, Na and Pb). For each element two linear fits were calculated. The first was based on all of the data that were within the linear range (these fits are shown in Fig. 1). The second was based on the last point contained in that curve and the first point not contained in that curve (*i.e.*, the first point for which nonlinearity was apparent). The concentration at which the interpolated (*i.e.*, calculated from the first curve) and extrapolated (*i.e.*, calculated from the second curve) emission calculated from these two curves

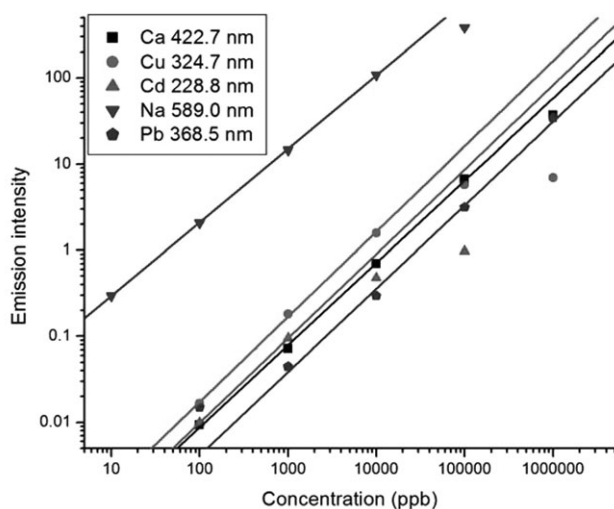


Fig. 1 Calibration plots for several elements. Lines are fits to the linear portions of the data.

differed by 5% was used to define the upper bound of the linear range. This, it should be noted, is a conservative estimate, as a curved line (the true shape) connecting the last two points will diverge rather slowly from the linear fit. Table 1 shows the limits of detection, approximate concentrations at which calibration curves become nonlinear (presumably due to self-absorption), and linear dynamic ranges based on these extremes.

Calibration plots for four of the elements have log–log plots with slopes very close to one, which would be expected from a perfectly linear relationship. The exception is sodium, the behavior of which can be explained as the result of an improper assumption that the only significant source of sodium is that which is intentionally added. In fact, our blanks have ppb-level sodium impurities. Adjusting the “known” concentrations upwards would result in a slope closer to one, but this adjustment was not made because the contaminant level in these particular samples is not known with sufficient certainty.

The linearity range varies from 2.0 (Cd) to at least 4.1 (Pb) orders of magnitude, which is an improvement on atomic absorption but is not as broad as ICP emission or ICP mass spectrometry. This relatively large linear range arises from the optical thinness of the source. An optically thin source has efficient emission (reflected in a high excitation temperature) from comparatively low atom concentrations and a short pathlength (narrow physical thickness). The ELCAD has both of these characteristics (> 5000 K Fe excitation temperature

Table 1 Working range details for several elements

Element	Wavelength/ nm	Slope of log–log plot	Detection limit/ppb	Upper bound/ ppm	Working range/ orders
Ca	422.7	0.956	20	110	3.7
Cu	324.7	0.990	30	11	2.6
Cd	228.8	0.980	10	1.1	2.0
Na	589.0	0.855	0.8	11	4.1
Pb	368.5	0.970	80	> 1000	≥ 4.1

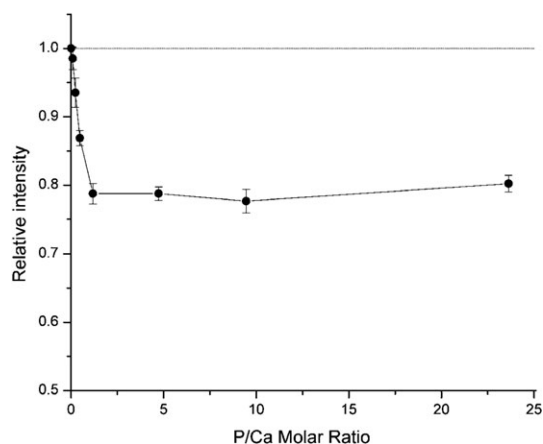


Fig. 2 Response of 422.7 nm emission to increasing amounts of phosphate (added as H_3PO_4). Upper line shows emission level with no phosphate present.

and 2 mm diameter). As in other emission-based techniques, the range can likely be expanded by using weaker lines at higher concentrations. It should be noted, however, that the sparse nature of ELCAD spectra, which was an advantage in the context of Section 1.1, is a disadvantage from this viewpoint.

3.2 Effect of phosphate on calcium

In some ways (*e.g.*, gas temperature), the ELCAD is more comparable to a chemical flame than to an ICP. Accordingly, interferences that are present in flame-based techniques are likely in the ELCAD. Chemical interferences, such as the binding of calcium by phosphate, are a notable example. To test for the presence of this interaction, a series of solutions with 2 ppm Ca and increasing amounts of phosphate was analyzed. The result is graphed in Fig. 2. The interference appears to take the same form as in a chemical flame, although it is less severe than in an air–acetylene flame under common conditions (*cf.* Smets²⁰). As phosphate concentration (added as H_3PO_4) is increased, calcium emission first drops, then levels off at about 79% relative to emission from the matrix-free sample. This leveling off takes place near a P : Ca molar ratio of 1 : 1, as in a flame.²⁰ The lesser magnitude of the effect here likely results in part from the higher gas temperature of ELCAD compared to air–acetylene flames.^{2,20}

Higher temperatures reduce the phosphate interference in flames. Accordingly, adjusting the ELCAD discharge current was tested as a remedy here. Two series of experiments were performed. One involved varying the current from 30 to 80 mA (30, 40, 55, 67 and 80 mA) while the blank-corrected emission from a solution of 2.5 ppm Ca and 27 ppm PO_4^{3-} (from H_3PO_4) was compared to that from a solution of 2.5 ppm Ca with no phosphate. The second used 20 ppm PO_4^{3-} (from Na_2HPO_4) and 2 ppm Ca with currents of 60, 80 and 100 mA. No trend or significant variation was seen within either data set. This is perhaps not surprising, since the rotational temperature (which is a good reflection of gas temperature) is not affected significantly by current in the ELCAD.²

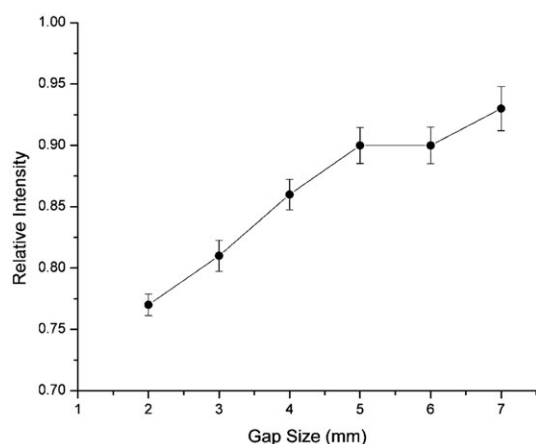


Fig. 3 Improvement in accuracy of calcium analysis in a 2.5 ppm Ca, 27 ppm PO_4^{3-} (added as H_3PO_4) solution with increasing gap size. Emission intensity at 422.7 nm is given relative to emission from at 2.5 ppm Ca solution with no PO_4^{3-} .

In chemical flames the gas temperature can be varied by using different oxidant/fuel combinations. In ELCAD, changing the gap has been shown to affect the rotational temperature.² Consequently, the effect of gap width on this interference was determined at a discharge current of 70 mA. Blank-subtracted emission from a solution of 27 ppm PO_4^{3-} (from H_3PO_4) and 2.5 ppm Ca was compared to that from a solution of 2.5 ppm Ca. The results are shown in Fig. 3. There is a reduction in the matrix effect as the gap is widened. Adjusting the gap could therefore potentially be used to diagnose the presence of a phosphate interference. For example, if the concentration calculated at a gap of 3 mm does not match the concentration calculated at a gap of 5 mm, the presence of an interferent can be assumed. Simply increasing the gap, however, does not seem a tenable solution to removing this interference. Even at a gap of 7 mm, which is more than twice what is typically used, a 7% suppression remains, and the rate of improvement appears to be declining. A more detailed study might reveal a reliably predictive relationship between the true concentration and the calculated concentrations at multiple gaps. Diagnostics, particularly one such as this that does not require adulterating the sample, are valuable in that they can be used to decide whether or not more time-consuming interference-reduction methods are necessary.

One such method is the addition of lanthanum. In flames, lanthanum is used to preferentially bind phosphate, thereby freeing calcium. To test this remedy, solutions of calcium; calcium and phosphate; calcium and lanthanum; and calcium, phosphate and lanthanum were prepared. When present, the concentrations were 2.5 ppm Ca, 27 ppm PO_4^{3-} , and 1000 ppm La. Lanthanum was added as $\text{La}(\text{NO}_3)_3 \cdot 6\text{H}_2\text{O}$, and phosphate was added as H_3PO_4 . Two blanks, one with 1000 ppm La and one with none, were also prepared. Reported values are the intensity of the sample minus the intensity of the relevant blank. The discharge gap for these experiments was 3.5 mm, and the current was 75 mA. In line with previous results, the solution with both calcium and phosphate produced 85% of the emission intensity of the

solution with calcium alone. The solution of calcium and lanthanum produced slightly less emission, 83% of the calcium-only solution. The solution of calcium, lanthanum and phosphate produced 99% as much emission as the calcium and lanthanum solution (82% as much as the calcium-only solution). The difference between the two lanthanum-containing solutions is within experimental error (1.4% difference compared to 1.8% (phosphate-containing) and 1.8% (phosphate-free) relative standard deviation), although it is possible that there is some small residual phosphate interference. It appears from these results that lanthanum, when present at high concentrations, also produces a matrix effect on calcium, so calibration curves must contain the same amount. At 1000 ppm, in addition to suppressing calcium emission by 17%, La reduced the background emission by 13% and the total voltage drop (including ballast resistor, discharge, and solution) by 3%. Although it was not examined in detail, this interference appears to be at least similar to the one discussed in Section 3.4.

The pattern of the effect with respect to phosphate concentration, the impact of temperature on the interference, and the alleviation of the suppression when lanthanum is added all point to similar origins in ELCAD and flames. It is likely, then, that the more general oxyanion interference with alkaline earth elements exists and can be remedied by conventional (for a flame) means.

3.3 Charge bias

To reach the negative glow, species from the solution must migrate towards a more positive potential. Since the elements analyzed by ELCAD are generally positively charged in solution, it is quite likely that the electric field impedes their migration. This is of concern primarily for two reasons. Most directly, a charge bias might exist where forms of the same element with different charges in solution would migrate into the plasma with different efficiencies, causing a biased emission signal and incorrect calculation of concentration. Further, the presence or absence of such a bias could inform the operational model. The charge difference need not be directly from the oxidation state of the element. In fact, because the solution pH is regulated and is held relatively low, oxidation state is probably a lesser concern than the difference in charge between “bare” atomic cations and metals covalently bound to other atoms. It is this difference that we chose to evaluate by comparing solutions of permanganate and dichromate to solutions with their respective metals as cations.

Three chromium standard curves were constructed, one each based on $\text{Cr}(\text{NO}_3)_3$, K_2CrO_7 , and $(\text{NH}_4)_2\text{CrO}_7$. The relative standard deviations of the slopes, in the same order, were 0.4, 0.5 and 0.9%. The slopes of the two Cr(vi)-based calibrations differed by 3%, which may have been due to a combination of enhancement by NH_4 and suppression by K (see Section 3.4). The slope of the Cr(III)-based curve was 13% lower than the average of the other curves.

To study the same effect with Mn, a 4 ppm solution of KMnO_4 was divided in two. Sodium bisulfite was added to one solution (enough to make the solution clear) to reduce the manganese to Mn(II) from Mn(VII). The Mn(VII) emission

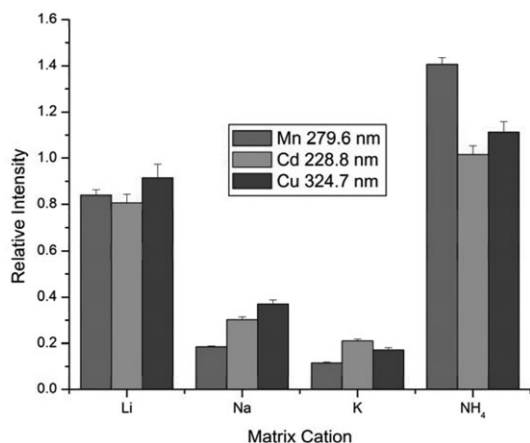


Fig. 4 Effect of equimolar (25 mM) concentrations of several chloride salts on analyte emission. Intensities have been corrected for blank emission. A relative intensity of 1 denotes absence of a matrix effect.

(which had a 0.9% RSD) was 16% more intense than the Mn(II) emission (which had a 0.5% RSD). While a Na matrix effect (see Section 3.4) might account for a few percent of this change, it does not account for most of it.

In both cases, the polyatomic anion containing a high oxidation state metal resulted in more emission per metal atom in solution than did the lower oxidation state atomic cation. The most apparent conclusion is that the species retain their charges, which hinder migration for positive ions but aid it for negative ions. Alternatively, or complementarily, cations may need to be neutralized prior to migration (for example, by oxide formation as argued by Cserfalvi and Mezei²¹), while anions can migrate with their charges intact.

The metals in the polyatomic anions obviously must be converted to free atoms before they can produce atomic emission. The observed emission trends imply that the increase in transport efficiency more than compensates for any loss in atomization efficiency, and/or atoms originating as atomic cations in solution are also bound (again, possibly as oxides) and must go through a similar atomization process.

3.4 Cation effects

The impact of only a few cations on emission of analytes and the discharge in general were studied in detail, but other cations appear to exhibit similar behavior (see Section 3.2 for evidence of analyte-emission suppression by high concentrations of lanthanum). Fig. 4 and 5 show the impacts of equimolar concentrations of several cations (introduced as chloride salts) on analyte emission and background emission, respectively. Emission was measured as the average of five 10-s measurements that have been corrected by subtraction of either the blank emission at the same wavelength with the same matrix (Fig. 4) or the dark signal (Fig. 5). This emission signal was then divided by an emission signal measured in the same way except without matrix in the solution. The plotted relative intensities are the results of this calculation. The error bars represent the error computed by propagating through the calculations the various standard deviations from the measurements.

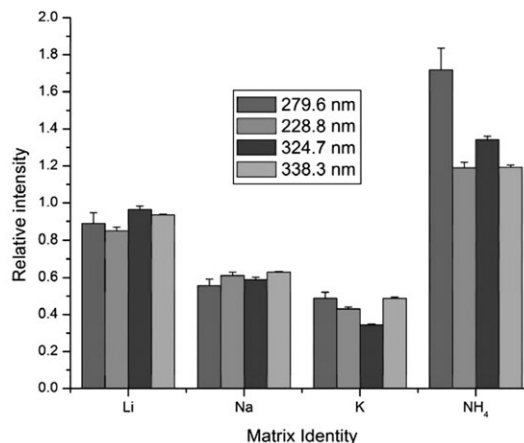


Fig. 5 Effect of equimolar (25 mM) concentrations of several chloride salts on background emission at several wavelengths. Intensities have been corrected for dark current. A relative intensity of 1 denotes absence of a matrix effect.

Notably, the continuum emission is suppressed or enhanced by approximately the same factor for a given matrix at every monitored wavelength. The suppression or enhancement of analyte emission by a given matrix is also similar for the metals observed. This clustering suggests methods for ameliorating the interference. Internal standards could certainly be used to lessen the inaccuracies, but there is enough scatter between elements that significant error would remain.

Other correction approaches might be found in the flexibility of the ELCAD system. Boosting the current, for example, intensifies emission. Two cadmium sample-blank pairs, one with 25 mM sodium and one without, were prepared. Emission from the matrix-free blank at the cadmium wavelength (228.8 nm) was recorded. Emission from the matrix-containing (but cadmium-free) solution was then monitored. The discharge current was adjusted until the background emission from the matrix-containing solution matched that of the matrix-free blank. This adjustment required a current of 110 mA, 38% higher than the original 80 mA. The emission from the solution containing both cadmium and sodium was next measured with the current at 110 mA and compared to the emission from the solution containing cadmium but not sodium with the current at 80 mA. With suitably reproducible wavelength accuracy or multiple detectors, this procedure could be simplified to omit the blanks. Without adjusting the current, the suppression was 70%. By adjusting the current, this error was reduced to 38%, which is still unacceptably large.

Related approaches might be more fruitful. For example, an internal standard could be combined with adjusting the current, with the idea that the emission from the standard would be restored at the same point as that of the analyte. As will be shown shortly, the power deposited across the discharge also drops in the presence of a matrix. Restoring this power by increasing the current to the appropriate level might also recover the analyte emission. Unfortunately, both of these approaches require the application of higher voltages than were available in this study.

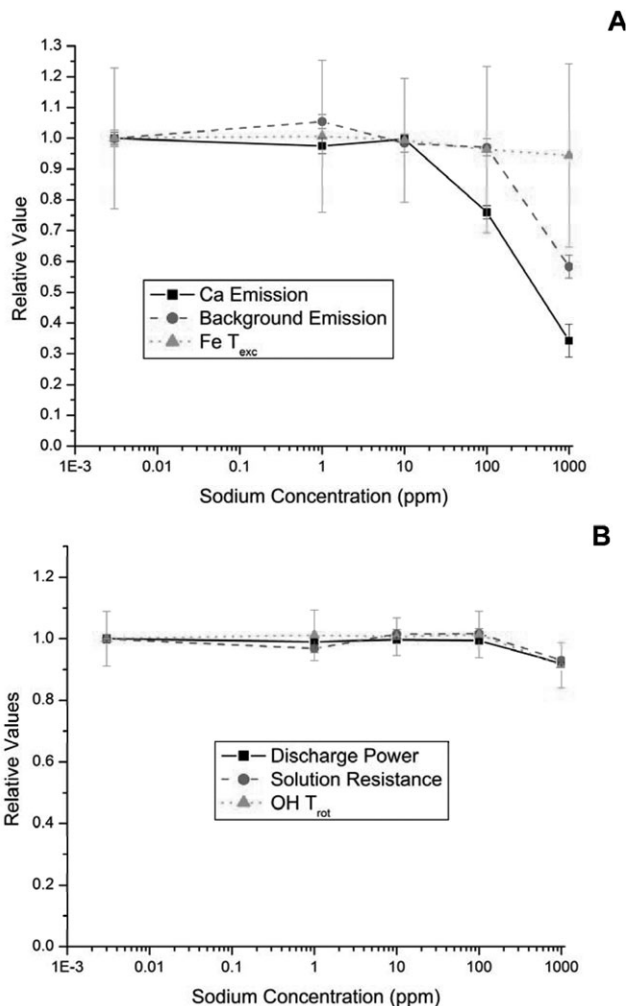


Fig. 6 Effect of matrix (Na) concentration on various discharge parameters. Calcium and background emission were measured at 422.7 nm. OH rotational and Fe excitation temperatures were calculated from Boltzmann plots such as in Fig. 7. Error bars represent one standard deviation.

Another fix would be to dilute the sample. Obviously, this requires that the suppression is less at lower matrix concentrations, and dilution comes at a cost to sensitivity. This was one reason for the next series of experiments, in which the effects of increasing sodium concentrations were measured. Another reason was to gain insight into the reason for the effect. To that end, parameters beyond just emission were monitored. Fig. 6 summarizes the results for a sodium matrix.

As Fig. 6 shows, six variables were monitored: Ca 422.7 nm emission, background emission at 422.7 nm, power deposited in the discharge, resistance across the solution, OH rotational temperature, and Fe excitation temperature. Several sets of solutions were used and not all measurements were made simultaneously. Sodium was introduced from a nitrate standard.

Iron was present (at approximately 10 ppm) only when its excitation temperature was being measured. This excitation temperature and the OH rotational temperature were both calculated from Boltzmann plots of a collection of lines.^{22,23} For OH, the lines were at 308.33, 308.52, 308.73, 309.53,

309.86, 311.02 and 311.48 nm. For Fe, they were at 371.99, 373.49, 373.71, 381.58, 382.04, 382.59, 383.42 and 385.99 nm. In both cases, the averages of peak areas from five spectra acquired by scanning the monochromator wavelength were used in the calculations.

Voltage probes were present only when solution resistance and discharge power were measured. These electrical characteristics were measured simultaneously with each other but separately from other factors. One probe was attached to the anode of the discharge. A second was attached to a wire that was inserted through the ELCAD capillary so that its bare tip was located just below the solution surface. The distance from the surface was well under 1 mm, but a more exact measurement is difficult because the solution level is lower when the discharge is on than when it is off. The voltage difference between the two probes was multiplied by the current to calculate the discharge power. The voltage between the solution probe and ground was divided by the current to compute the solution resistance. Admittedly, both measurements will be somewhat off because of the small distance between the solution-probe tip and the solution surface. However, this error does not seem to be substantial and should be consistent among measurements.

Ten 10-s measurements were averaged for each Ca emission data point. Matrix-matched blanks (also taken from ten 10-s measurements) were used for background correction. These same blank-corrected measurements were used to monitor background emission. In this latter case, a 300-s dark measurement (with the plasma extinguished) was subtracted before the results were plotted.

As Fig. 6 shows, all six factors are constant, or nearly so, through 100 ppm Na, except for Ca emission and the Fe excitation temperature. At 1000 ppm, however, all of the measured values drop. Ca emission declines the most substantially, down to 66% lower than in a matrix-free situation. Background emission falls by a lesser 32%. Other factors go down by a lower, but fairly uniform, approximately 10%.

The observed matrix effect is likely to arise from a mixture of sources, so several that are consistent with the evidence will be discussed below.

Solution resistance can be expected to correlate with energy lost to the solution as heat. In the cell design used here, the pipette that delivers the sample solution passes through the waste reservoir, which allows the solution to be heated before reaching the discharge. The small cross-sectional area of the overflow connecting the discharge to the waste reservoir is responsible for the bulk of the solution resistance² and is therefore an area of high resistive heating. It has been shown that heating the solution results in higher ELCAD emission.²⁴ A possible explanation is that heating lowers the surface tension and improves transport into the discharge and/or results in smaller droplets that can be more readily desolvated. High matrix concentrations lower the solution resistance and the solution heating, which should decrease transport and/or desolvation efficiency.

Introducing large amounts of a metal, particularly one as easily ionizable as sodium, is likely to raise electron and ion populations in the plasma. To check this hypothesis, the half-width of the 486.1 nm hydrogen-beta line was measured for

two conditions: a blank solution and a solution containing 500 ppm sodium (which is close in concentration to the 25 mM solution used earlier). With the monochromator slits narrowed to 10 μm (giving 15 pm resolution), emission was collected at 30 pm intervals over a 643 pm window symmetrically encompassing the H_β peak. The points were collected in two passes as a check against drift (none was apparent). For the blank solution, a 30-s average of data collected at 1 kHz was used for each point. This time was increased to 50 s for the matrix-containing solution in anticipation of weaker signals. In fact, once the baseline was subtracted, the signals were comparable in magnitude. The peaks have Voigt profiles but are dominated by Lorentzian character. Origin (OriginLab Corporation, Northampton, MA) was used to fit the two peaks to Lorentzian curves. The full widths at half maximum (FWHM) computed by the program were 148 and 184 pm for the matrix-free and matrix-containing solutions, respectively. Calculating exact electron number densities from these widths is not possible because there are several factors that are not controlled. Notably, other sources of broadening have not been compensated, and the measurement is not restricted to a single spatial location. Vertically, both the negative glow and a portion of the positive column (which have significantly different electron number densities¹²) are included, and no attempt at radial resolution was made. With those caveats in mind, it seems worthwhile to obtain a crude estimate of the difference in electron number densities. Interpolating from tables,²⁵ we calculate number densities of $6.5 \times 10^{14} \text{ cm}^{-3}$ in the absence of matrix and $8.9 \times 10^{14} \text{ cm}^{-3}$ with 500 ppm sodium. This increase is substantial, but its precise magnitude should be treated with some skepticism for the above-mentioned reasons.

Whether or not it is by 37%, it is clear that there is some elevation in electron number density caused by Na. This change would be expected to reduce the plasma resistance, and therefore the power deposited in it. Indeed, with 1000 ppm sodium, an 8.8% drop in discharge power is observed relative to the power with lower Na concentrations. With less power deposited, the OH rotational temperature also drops by 8% (from 2980 to 2730 K).

The behavior of the Fe excitation temperature (Fig. 6(a)) stands out from other factors. This temperature appears to drop only slightly, rather than showing an abrupt change. The rather large errors associated with spectroscopic temperature measurements, however, caution against too much weight being given to the small changes observed. Even the change between the temperature above the matrix-free solution (5930 K) and the 1000 ppm Na solution (5600 K) might not be real. Assuming it is, this 6% change in excitation temperature is not enough to account for the drop in calcium emission, but looking more deeply into the measurements is revealing. Fig. 7 shows the Boltzmann plots used to calculate the excitation temperature. The slopes of such plots and excitation temperature are inversely proportional. The degree of scatter, and its potential effect on the slopes, support caution in giving too much credence to the small changes in temperature that were calculated. The highest sodium concentration curve stands out, however, not because of its slope, but because of its offset.

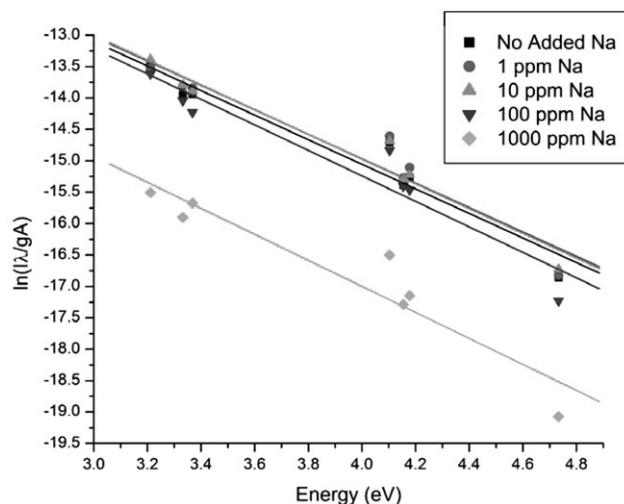


Fig. 7 Boltzmann plots used to determine iron excitation temperatures at different concentrations of sodium.

The y -intercept of each plot in Fig. 7 is proportional to:

$$\ln \left[\frac{nlhc}{4\pi Z(T)} \right]$$

where l is the path length of the source, h is Planck's constant, and c is the velocity of light. Only n (the atom number density) and $Z(T)$ (the partition function) are not constant. Given the excitation temperature, the partition function can be calculated from polynomial equations given by Irwin.²⁶ Solving for the relative number densities shows that the atom population drops substantially (by 77%) in the plasma above the solution with the highest matrix concentration (1000 ppm) relative to the Na-free solution. For the other samples, atom populations vary by $\pm 6.5\%$ relative to their average, with no directionality to the trend. Given that the relative standard deviations calculated from the least-squared fits vary between 11 and 15%, only the difference between the 1000 ppm solution and the others is significant. More detail is provided in Table 2.

Also shown in Table 2 are the results of a further analysis. We can back-calculate the relative intensities of the lines used in the original calculation from the equation:

$$\frac{I}{I_0} = \left(\frac{n}{n_0} \right) \left(\frac{Z(T_0)}{Z(T)} \right) \exp \left(\frac{E_p}{kT_0} - \frac{E_p}{kT} \right)$$

where E_p is the excitation energy of the level from which the emission occurs and I is the intensity of that emission. Terms

Table 2 Evaluation of excitation and concentration (transport) components of observed Fe emission in Na matrix. See text for basis of computations

Sodium concentration/ppm	Average emission	Excitation component	Concentration component
0	1.00	1.00	1.00
1	1.09	1.04	1.05
10	1.09	0.96	1.14
100	0.84	0.77	1.09
1000	0.15	0.67	0.22

subscripted with zero refer to the condition with no added matrix, and terms without subscripts refer to the condition with matrix (n , I and T) or are not a function of matrix (E_p and k). More importantly, we can use the same equation to determine the relative contributions of concentration and excitation to the observed variation. The term in the left-most brackets is the relative atom population. The remainder of the right side of the equation is the relative emission efficiency, which is temperature-based. The product of the two terms, as the equation shows, is the relative emission intensity (I/I_0). To simplify the comparison, the relative values for all seven emission lines for a given solution were averaged. These averages are reported in Table 2. The contribution from concentration is relatively steady through 100 ppm, but drops dramatically (down to 22% of the original) at 1000 ppm. Clearly, the high concentration of Na has reduced the Fe population in the discharge. The excitation component drops more gradually and less severely (to 67% of the original at 1000 ppm). Again, the degree of temperature change is very uncertain.

Combined, the above results suggest that the observed matrix effect can be divided into excitation and transport. The components have already been sketched, but they will be restated based on the combined evidence.

A likely mechanism for the excitation effect starts with the introduction of an easily ionized element into the plasma. Through an increase in ion and electron populations, the discharge becomes more conductive. With less resistance, the amount of energy deposited in the plasma is reduced. Lower power leads to a cooler and generally less energetic plasma.

“Transport” is used rather broadly here to refer to the combined processes involved in converting an atom in solution to a free atom in the discharge. Evidence suggests that, just as in other plasmas, this process could be further divided into droplet formation, desolvation, vaporization and atomization. The latter three steps are tied into the same mechanism as the excitation effects. A cooler plasma will be less efficient at desolvation, vaporization, and atomization.

The magnitude of the transport effect (a 78% reduction at a Na concentration of 1000 ppm) makes us believe that there is more to it than just a change in the plasma energy. It seems likely that aerosol droplet formation is also affected. The mechanism of droplet formation in the ELCAD has not yet been clearly established, but solution viscosity should influence the ease of droplet formation and the droplet size. High salt concentrations reduce solution heating by increasing conductance. Cooler solutions are more viscous, and would be expected to produce larger droplets that are more difficult to desolvate.

There may be further transport effects. An important clue to the ELCAD mechanism is that desolvation, vaporization, and atomization proceed to a significant degree in a very small space. Emission for many elements peaks well within a millimeter from the solution surface, in the negative glow.^{2,8} The velocity of analyte species leaving the solution and the size of the droplets containing those analytes are both unknown, so the residence time cannot be calculated. It seems unlikely, however, that the observed level of desolvation could take place in this short space by a purely thermal mechanism. Between the solution and the negative glow is the cathode fall, where there is a large potential drop in a small space.

Cserfalvi and Mezei estimate the field in this region to be on the order of 10^7 V m⁻¹.²¹ Passing initially neutral droplets through high fields has been used to decrease the mean droplet size.^{27,28} As we have shown, this matrix effect lowers the field strength, which would be expected to hamper this mode of desolvation. Of course, droplets from the ELCAD cathode may not be initially neutral. The situation might be similar to electrospray, where droplets are initially charged, helping to liberate them from the solution.

Thoroughly explicating this possibility would be beyond the scope of the present paper, but some exploration of the implications is appropriate. Solution surface roughness caused by boiling could result in high local fields, possibly as high as would be needed for charged-droplet ejection. If so, the temperatures at this interface could influence the surface roughness and therefore droplet formation. The surface-tension effect explained earlier is also consistent with this mechanism. Field strength would affect both droplet formation and desolvation. Ion concentration in the solution would also impact the efficiency of droplet formation, and competitive effects might reduce analyte concentration in droplets when a high cation concentration is present. In fact, an electrospray-like mechanism might explain at least part of the strong dependence of emission on electrolyte identity and concentration (see Section 1.3).

4 Conclusions

A variety of potential complications to the use of ELCAD for the analysis of complex solution have been considered. A number of interferences have been shown to be either minimal or easily remedied, but others remain significant. The worst matrix effect arises from high concentrations of cations. This problem can be easily diagnosed by the reduction in background emission and the presence of strong emission from the interferences. This diagnostic aid is simple to implement in an emission-based system such as the present one, where wavelength can readily be scanned or in one where multiple wavelengths can be monitored simultaneously. The response of the ELCAD to these interferences provides clues to a possible mechanism, in which droplet formation and desolvation are both enhanced by the strong electric field of the cathode fall and in which the discharge temperature is altered. Overall, previous literature in which interferences in flames are examined serves as a useful preliminary guide to gauging similar effects in the ELCAD.

Acknowledgements

This work was supported in part by the US Department of Energy through Grant DE-FG02-98ER14890. The authors are grateful to SPEX CertiPrep for providing standard solutions and to G. C.-Y. Chan for providing the program for the calculation of partition functions.

References

- 1 T. Cserfalvi, P. Mezei and P. Apai, *J. Phys. D: Appl. Phys.*, 1993, **26**, 2184–2188.

- 2 M. R. Webb, F. J. Andrade, G. Gamez, R. McCrindle and G. M. Hieftje, *J. Anal. At. Spectrom.*, 2005, **20**, 1218–1225.
- 3 T. Cserfalvi and P. Mezei, *J. Anal. At. Spectrom.*, 2003, **18**, 596–602.
- 4 T. Cserfalvi and P. Mezei, *J. Anal. At. Spectrom.*, 1994, **9**, 345–349.
- 5 T. Cserfalvi and P. Mezei, *Fresenius' J. Anal. Chem.*, 1996, **355**, 813–819.
- 6 P. Mezei, T. Cserfalvi and M. Janossy, *J. Anal. At. Spectrom.*, 1997, **12**, 1203–1208.
- 7 M. A. Mottaleb, Y. A. Woo and H. J. Kim, *Microchem. J.*, 2001, **69**, 219–230.
- 8 P. Mezei, T. Cserfalvi and L. Csillag, *J. Phys. D: Appl. Phys.*, 2005, **38**, 2804–2811.
- 9 P. Mezei, T. Cserfalvi, M. Janossy, K. Szocs and H. J. Kim, *J. Phys. D: Appl. Phys.*, 1998, **31**, 2818–2825.
- 10 G. C. Y. Chan and G. M. Hieftje, *Spectrochim. Acta, Part B*, 2004, **59**, 163–183.
- 11 V. D. Hodoroba, V. Hoffmann, E. B. M. Steers and K. Wetzig, *J. Anal. At. Spectrom.*, 2000, **15**, 951–958.
- 12 M. R. Webb, G. C. Y. Chan, F. J. Andrade, G. Gamez and G. M. Hieftje, *J. Anal. At. Spectrom.*, 2006, **21**, 525–530.
- 13 Y. S. Park, S. H. Ku, S. H. Hong, H. J. Kim and E. H. Piepmeier, *Spectrochim. Acta, Part B*, 1998, **53**, 1167–1179.
- 14 J. M. Mermet, in *Inductively Coupled Plasma Spectrometry and its Applications*, ed. S. J. Hill, Sheffield Academic Press, Sheffield, 1999.
- 15 P. Mezei, T. Cserfalvi, H. J. Kim and M. A. Mottaleb, *Analyst*, 2001, **126**, 712–714.
- 16 V. V. Yagov and M. L. Gentsina, *J. Anal. Chem.*, 2004, **59**, 64–70.
- 17 E. Beinrohr, P. Csemi and J. F. Tyson, *J. Anal. At. Spectrom.*, 1991, **6**, 307–311.
- 18 M. A. Taher, *Analyst*, 2000, **125**, 1865–1868.
- 19 M. Sperling, Z. L. Fang and B. Welz, *Anal. Chem.*, 1991, **63**, 151–159.
- 20 B. Smets, *Analyst*, 1980, **105**, 482–490.
- 21 T. Cserfalvi and P. Mezei, *J. Anal. At. Spectrom.*, 2005, **20**, 939–944.
- 22 Y.-i. Sung and H. B. Lim, *J. Anal. At. Spectrom.*, 2003, **18**, 897–901.
- 23 U. Engel, C. Prokisch, E. Voges, G. M. Hieftje and J. A. C. Broekaert, *J. Anal. At. Spectrom.*, 1998, **13**, 955–961.
- 24 V. A. Titov, V. V. Rybkin, A. I. Maximov and H. S. Choi, *Plasma Chem. Plasma Process.*, 2005, **25**, 503–518.
- 25 R. A. Hill, *J. Quant. Spectrosc. Radiat. Transfer*, 1964, **4**, 857–861.
- 26 A. W. Irwin, *Astrophys. J., Suppl. Ser.*, 1981, **45**, 621–633.
- 27 D. B. Hager and N. J. Dovichi, *Anal. Chem.*, 1994, **66**, 1593–1594.
- 28 R. N. Savage and G. M. Hieftje, *Rev. Sci. Instrum.*, 1978, **49**, 1418–1424.